Clin Orthop Relat Res (2019) 477:159-174
DOI 10.1097/CORR.0000000000000535

Clinical Orthopaedics and Related Research®
A Publication of The Association of Bone and Joint Surgeons®

Clinical Research

MRI of THA Correlates With Implant Wear and Tissue Reactions: A Cross-sectional Study

Matthew F. Koff PhD, Christina Esposito PhD, Parina Shah MS, Mauro Miranda MFA, Elexis Baral BS, Kara Fields MS, Thomas Bauer MD, PhD, Douglas E. Padgett MD, Timothy Wright PhD, Hollis G. Potter MD

Received: 21 March 2018 / Accepted: 1 October 2018 / Published online: 26 November 2018
Copyright © 2018 by the Association of Bone and Joint Surgeons

Abstract

Background MRI is predictive of adverse local tissue reactions (ALTRs) after THA but how MRI directly relates to implant surface wear, fretting, and trunnion corrosion at different articulations between implant components remains unclear. MRI generates high-contrast images to display soft tissues around arthroplasty and may provide a

One of the authors certifies that she (HGP), or a member of her family, has received or may receive payments or benefits, during the study period, an amount of more than USD 1,000,000 from General Electric Healthcare (Waukesha, WI, USA). One of the authors certifies that he (MFK), or a member of his immediate family, has received or may receive payments or benefits, during the study period, an amount of USD 100,001 to USD 1,000,000 from Johnson and Johnson (New Brunswick, NJ, USA). One of the authors certifies that he (TB), or a member of his immediate family, has received or may receive payments or benefits, during the study period, an amount of less than USD 10,000 from Stryker Orthopaedics (Kalamazoo, MI, USA), an amount of less than USD 10,000 from Acumed (Hillsboro, OR, USA), an amount of USD 10,000 to 100,000 from Leica Biosystems (Buffalo Grove, IL, USA), an amount of less than USD 10,000 from Spinal Dynamics (Mercer Island, WA, USA), and an amount of 10,000 to 100,000 from the *Journal of Bone and Joint Surgery* (Needham, MA, USA). One of the authors certifies that he (TW), or a member of his immediate family, has received or may receive payments or benefits, during the study period, an amount of more than USD 1,000,001 from the Mary and Fred Trump Institute for Implant Analysis at the Hospital for Special Surgery (New York, NY, USA). One of the authors certifies that he (DEP), or a member of his immediate family, has received or may receive payments or benefits, during the study period, an amount of USD 10,000 to 100,000 from DJO Global (Vista, CA, USA). Research reported in this publication was supported by the National Institute of Arthritis and Musculoskeletal and Skin Diseases of the National Institutes of Health under award number R01AR064840 (Co-Principal Investigators: MFK, HGP).
Clinical Orthopaedics and Related Research® neither advocates nor endorses the use of any treatment, drug, or device. Readers are encouraged to always seek additional information, including FDA approval status, of any drug or device before clinical use.
Each author certifies that his or her institution approved the human protocol for this investigation and that all investigations were conducted in conformity with ethical principles of research.
The content of this article is solely the responsibility of the authors and does not necessarily represent the official views of the National Institutes of Health.

M. F. Koff, P. Shah, M. Miranda, H. G. Potter, MRI Research Laboratory, Hospital for Special Surgery, New York, NY, USA

C. Esposito, E. Baral, T. Wright, Department of Biomechanics, Hospital for Special Surgery, New York, NY, USA

K. Fields, Healthcare Research Institute, Hospital for Special Surgery, New York, NY, USA

T. Bauer, Department of Pathology and Laboratory Medicine, Hospital for Special Surgery, New York, NY, USA

D. E. Padgett, Adult Reconstruction and Joint Replacement Division, Hospital for Special Surgery, New York, NY, USA

M. F. Koff (✉), Hospital for Special Surgery, 535 East 70th Street, New York, NY 10021, USA, email: koffm@hss.edu

All ICMJE Conflict of Interest Forms for authors and *Clinical Orthopaedics and Related Research*® editors and board members are on file with the publication and can be viewed on request.

Wolters Kluwer

Copyright © 2018 by the Association of Bone and Joint Surgeons. Unauthorized reproduction of this article is prohibited.

surgeon the means to distinguish and differentiate host-related synovial patterns as a response to either polyethylene wear or metal wear and corrosion products.

Questions/purposes The purposes of this study were (1) to correlate findings from MRI in patients who have undergone THA with direct assessment of implant wear, corrosion, and fretting from retrieved components; and (2) to distinguish the unique synovial responses on MRI in patients who have undergone THA based on bearing materials.

Methods In this prospective study, patients undergoing THA (181 patients, 187 hips) with metal-on-metal (MoM), hip resurfacing (HRA), metal-on-polyethylene (MoP), ceramic-on-polyethylene, ceramic-on-ceramic, or modular neck designs having revision surgery (between October 2013 and June 2017) underwent preoperative MRI. A single reader blinded to the bearing surface made an assessment of the synovial response (Gwet's AC1, 0.65-0.97); these data were compared with semiquantitative histology of tissue samples by a single reader (Gwet's AC1, 0.92) and semiquantitative wear, corrosion, and fretting analysis of retrieved components using Goldberg scoring (Gwet's AC1, 0.60-0.79). Direct noncontact measurements of implant wear were also made. Correlations and analyses of variance were used to assess associations between metrics and differences by implant type, respectively.

Results Correlations were found between MRI synovial thickness with severity of fretting and corrosion damage of the female head-neck trunnion of femoral stems in modular designs (ρ = 0.26 [95% confidence interval {CI}, 0.12-0.39]; p = 0.015, n = 185) and ALTR grade and volumetric wear in MoM bearings (ρ = 0.93 [95% CI, 0.72-0.98]; $p < 0.001$, n = 10). MRI synovial thickness was highest in patients identified with aseptic lymphocyte-dominated vasculitis-associated lesions and diffuse tissue necrosis. On MRI, MoP hips demonstrated a distinct polymeric synovial response, whereas HRA, MoM, and modular hips more commonly demonstrated ALTR. Hips classified as having a polymeric synovial response on MRI had a greater number of particles present in tissue samples.

Conclusions In this study, we demonstrated that MRI of THA can distinguish synovial responses that reflect the bearing type of the implanted THA and correlate to direct measurements of implant wear, corrosion, and fretting and histologic assessment of wear particles in periprosthetic tissues. MRI provides a means of direct, noninvasive visualization of the host-generated synovial response. Patients presenting with painful arthroplasties may be evaluated for the cause of their discomfort, specifically highlighting any concerning synovial reactions that would warrant more prompt surgical intervention. Future studies would benefit from a prospective evaluation of different implants to assess the natural longitudinal history of arthroplasty complications, including the development and prevalence of ALTR across bearing constructs.

Level of Evidence Level III, diagnostic study.

Introduction

Osteolysis after THA has been markedly reduced with the introduction of highly crosslinked polyethylene [4]; however, revision surgery caused by problems arising from the materials used in the bearing couple is still necessary. Ceramic and metal bearing surfaces were developed to reduce wear, osteolysis, and loosening [1]. Ceramic-on-ceramic (CoC) bearings have low wear rates but may chip, fracture, or squeak [11]. Metal-on-metal (MoM) THA and hip resurfacing arthroplasty (HRA) designs can have annual linear wear rates less than metal-on-polyethylene (MoP) articulations [46] but produce more [15] and smaller wear debris [20]. Wear debris can also be generated from the femoral head-neck taper in THA or at the neck-stem taper in dual modular stem designs. Debris from modular tapers have been implicated in severe adverse local tissue reactions (ALTRs) [3], commonly referred to as metal debris in surrounding tissues [28], soft tissue destruction [53], or the presence of a "pseudotumor" [41].

Previous researchers have used MRI extensively to evaluate ALTRs, but these studies have focused primarily on MoM or modular designs [16, 26, 45]. Recently, investigating mechanically assisted crevice corrosion in MoP has drawn interest among arthroplasty surgeons [12] as a result of the associated presence of ALTRs, and MRI has been effective for the preoperative assessment of corrosion in patients undergoing MoP THA [10, 35, 40]. MRI for the evaluation of ALTRs has also been applied to ceramic-on-polyethylene (CoP) constructs [5]. Historically, MRI of THA has been challenging because distortions caused by the metallic components of the THA are seen in generated images [24]; however, new metal artifact reduction sequences, specifically, multispectral imaging (MSI) such as multiacquisition variable resonance image combination (MAVRIC) [23] and others [30], mitigate these distortions. A limitation of some of these studies is the lack of utilization of MSI sequences to assess ALTRs [7]; furthermore, most MRI grading protocols typically assign a classification based on visual assessment of the structures surrounding THA. Even with the high variability of these MRI grading methods [2, 50], the location of ALTR has been correlated with ALTR morphology (wall thickness) [18]. A limitation of these MRI protocols is a lack of a direct correlation to clinically or biologically relevant findings [17, 18, 33, 51] and direct wear measurements. One previous study evaluated the relationship between MRI visualization of ALTR and subsequent retrieval analysis but focused on a single recalled modular system [37]. Given the soft

Copyright © 2018 by the Association of Bone and Joint Surgeons. Unauthorized reproduction of this article is prohibited.

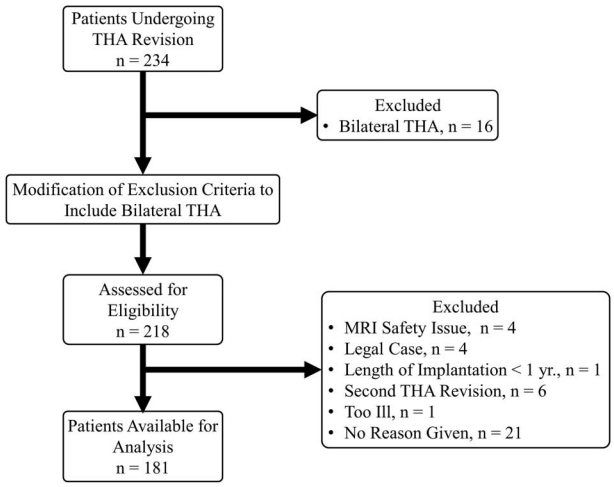

Fig. 1 A STROBE flow diagram demonstrates patient recruitment during the study time period.

tissue damage and poor outcomes associated with ALTRs, a need exists for an imaging modality that can noninvasively distinguish the synovial response in patients independent of the bearing materials. A patient with a MoP implant may have an ALTR related to tribocorrosion, which may warrant more immediate consideration for revision, as opposed to a more "benign" polymeric synovitis.

Therefore, the purposes of this study were (1) to correlate findings from MRI in patients who have undergone THA with direct assessment of implant wear, corrosion, and fretting from retrieved components; and (2) to distinguish the unique synovial responses on MRI in patients who have undergone THA based on bearing materials.

Materials and Methods

This prospective study had local institutional review board approval. Between October 2013 and June 2017, 234 patients underwent revision of MoM, HRA, CoP, CoC, and metal-on-polyethylene (MoP) modular neck designs at one center (Fig. 1). Of those, 181 (77%; Table 1) were enrolled in this study. Inclusion criteria were the patient was undergoing revision of primary THA with "revision" defined as an open procedure with change or exchange of any component and preoperative MRI was available for evaluation. The exclusion criterion was patients undergoing MoP THA with < 1 year of implantation. Patients with bilateral THAs were initially part of the exclusion criteria to prevent difficulties in interpreting blood serum metal ion levels, but the exclusion criterion was modified as a result of the limited enrollment of patients undergoing unilateral surgery. Patients met inclusion if undergoing primary revision of one of five implant designs: MoM (n = 35), HRA (n = 18), ceramic articulations (CoP [n = 26] or CoC [n = 6]), MoP with > 1 year of implantation (n = 58), and modular neck designs (MoP [n = 37], CoP [n = 5], CoC [n = 1], ceramic-on-metal [CoM, n = 1]). All patients were a minimum of 1 year postimplantation, except participants with modular neck designs as a result of a recalled implant (n = 6). Information regarding the retrieved implant designs and reason for revision is provided (Appendix, Supplemental Digital Content). The length of implantation (LOI) varied by implant. Patients receiving MoP implants had the longest LOI. LOI of MoM (7 [2], mean [SD]) was not different from HRA (7 [3], p = 0.811) and was longer than modular designs (5 [4], p < 0.001), CoP (6 [6], p = 0.005) but shorter than MoP (12 [8], p = 0.016). Patient age varied by implant type (p < 0.001) with patients undergoing MoP THA older than those undergoing HRA (MoP: 66 [13], HRA: 53 [10], p < 0.001) and CoP (57 [14], p = 0.002). Patients undergoing MoM THA were older than those undergoing HRA (MoM: 60 [9], HRA: 53 [10], p = 0.021).

Preoperative blood draws were performed on all patients to evaluate serum cobalt and chromium, regardless of THA design (Arup Laboratories, Salt Lake City, UT, USA). All testing was performed using standard institutional methods. We sought to use the previously

Table 1. Demographics by implant type

Parameter	MoM THA (n = 35)	HRA (n = 18)	Modular designs (n = 44)	MoP THA (n = 58)	CoP THA (n = 26)	CoC THA (n = 6)	p value
Age* (years)	60 (9)	53 (10)	64 (10)	66 (13)	57 (14)	59 (8)	< 0.001
Sex							0.91
Male†	19 (54%)	7 (39%)	20 (45%)	28 (48%)	11 (42%)	3 (50%)	
Female†	16 (46%)	11 (61%)	24 (55%)	30 (52%)	15 (58%)	3 (50%)	
Body mass index* (kg/m^2)	28 (5)	26 (5)	28 (5)	26 (5)	26 (5)	33 (6)	0.008
Length of implantation*	7 (2)	7 (3)	5 (4)	12 (8)	6 (6)	5 (4)	< 0.001

*Values displayed as mean (SD).
†values displayed as count (percentage); MoM = metal-on-metal; HRA = hip resurfacing arthroplasty; MoP = metal-on-polyethylene; CoP = ceramic-on-polyethylene; CoC = ceramic-on-ceramic.

Copyright © 2018 by the Association of Bone and Joint Surgeons. Unauthorized reproduction of this article is prohibited.

Table 2. Metal ion levels for patients with unilateral THA

Parameter	MoM THA (n = 14)	HRA (n = 12)	Modular designs (n = 24)	MoP THA (n = 27)	CoP THA (n = 16)	CoC THA (n = 1)	p value
Cobalt levels (μg/L)	7.7 (4.6-19.6)	5.0 (1.7-28.1)	5.5 (1.7-10.0)	0.0 (0.0-1.0)	0.0 (0.0-0.0)	0.0 (0.0-0.0)	< 0.001
Chromium levels (μg/L)	9.0 (1.5-11.8)	5.0 (1.4-41.1)	1.6 (0.0-2.3)	0.0 (0.0-1.0)	0.0 (0.0-0.0)	0.0 (0.0-0.0)	< 0.001

Values displayed as median (interquartile range); MoM = metal-on-metal; HRA = hip resurfacing arthroplasty; MoP = metal-on-polyethylene; CoP = ceramic-on-polyethylene; CoC = ceramic-on-ceramic.

published methods described by MacDonald et al. [31]; however, serum data were obtained for a majority of the patients undergoing MoM THA and HRA before study enrollment. The remaining patients had serum obtained through intravenous acquisition at the time of surgery with blood draw into glass tubes. Analysis of serum ion levels utilized only patients undergoing unilateral THA (n = 94) to minimize confounding influences from bilateral THAs. Cobalt and chromium levels differed by implant type (Table 2). Metal bearing surfaces and modular designs had elevated cobalt levels (MoM [7.7 {4.6-19.6} μg/L] and HRA [5.0 {1.7-28.4} μg/L], median [interquartile range]) and chromium levels (MoM [9.0 {1.5–11.8} μg/L] and HRA [5.0 {1.4–41.1} μg/L]) as compared with MoP ($p = 0.003$, cobalt: 0.0 [0.0–1.0] μg/L and chromium: 0.0 [0.0–1.0] μg/L). MoM also had greater cobalt and chromium levels than CoP ($p < 0.003$, cobalt: 0.0 [0.0–0.0] μg/L and chromium: 0.0 [0.0–0.0] μg/L). Weak to moderate correlations were found between cobalt and chromium levels and MRI synovial thickness ($\rho = 0.50$ [95% confidence interval {CI}, 0.33-0.64]; $p < 0.001$ and $\rho = 0.41$ [95% CI, 0.23-0.57]; $p = 0.001$, respectively) and between cobalt and chromium levels and MRI synovial volume ($\rho = 0.29$ [95% CI, 0.09-0.46]; $p = 0.005$ and $\rho = 0.21$ [95% CI, 0.00-0.39]; $p = 0.046$, respectively). Strong correlations were found between acetabulum volumetric wear and cobalt ($\rho = 0.90$ [95% CI, 0.09-0.99]; $p = 0.037$) and chromium ($\rho = 0.90$ [95% CI, 0.09-0.99]; $p = 0.037$) levels and between femoral head volumetric wear and chromium ($\rho = 0.89$ [95% CI, 0.18-0.99]; $p = 0.015$) levels. A similar trend was found between femoral head volumetric wear and cobalt levels ($\rho = 0.77$ [95% CI, -0.11 to 0.97]; $p = 0.076$). Cobalt levels correlated with visual damage of the femoral head female trunnion in MoP ($\rho = 0.53$ [95% CI, 0.18-0.76]; $p = 0.005$) and with the femoral stem male trunnion in MoP ($\rho = 0.89$ [95% CI, 0.05-0.99]; $p = 0.043$).

Preoperative MRI was performed on clinical 1.5-T scanners (GE Healthcare, Waukesha, WI, USA) with an eight-channel phased-array cardiac coil (GE Healthcare). Three-plane two-dimensional fast-spin echo images and coronal MAVRIC-SL and MAVRIC-SL STIR images (Table 3) were evaluated by two radiologists (HGP, AJB), one of whom is a musculoskeletal radiologist with > 20 years of experience of imaging near arthroplasty. The images were evaluated for the presence of synovitis (yes/no), type of synovitis (predominantly fluid signal intensity, solid particulate debris [17], or mixed fluid and particulate debris [37]), classification of synovium: (1) normal = thin capsule with low signal intensity [44]; (2) ALTR = thickened, hyperintense capsule, often with a poor zone of demarcation from the muscle signal and architecture of the surrounding muscle and soft tissues envelope, indicating necrosis [38]; (3) metallosis = low signal intensity deposits located in the capsular lining within the joint or in an extracapsular location, infection = lamellated synovial lining with pericapsular edema [43]; (4) polymeric = intracapsular foci of particulate, intermediate signal intensity debris [44]; and (5) mildly abnormal, maximal inferomedial synovial thickness in the coronal plane, synovial volume, presence of synovial decompression, and ALTR grade (none, mild, moderate, severe). A single characterization of the soft tissues, assigned by the synovial classification, was used to facilitate subsequent statistical comparisons. All grading was performed in a blinded fashion to implant design and composition, corresponding radiographs, subsequent histology, implant wear, and corrosion data. A second musculoskeletal radiologist (AJB) with 10 years of experience independently evaluated all images to assess repeatability of the synovial classification. Gwet's AC1 was used to assess inter- and intrarater agreement of MR synovial classification between the two readers and found an interrater agreement of substantial to almost perfect (AC1 range, 0.65-0.97) and an intrarater agreement of moderate to almost perfect (AC1 range, 0.59-0.99).

Preoperative imaging was also used to identify locations of interest for intraoperative tissue sampling. Tissue samples (approximately 5 cm^3) of the synovium were acquired based on the preoperative MRI. Tissue samples were fixed in 10% buffered formalin for 24 hours, processed, embedded, and cut following standard procedures. Sections from each block were stained with hematoxylin and eosin. The tissue samples were evaluated by a board-certified pathologist (TB) with > 20 years of experience evaluating soft tissue near arthroplasty using Campbell's aseptic lymphocyte-dominated vasculitis-associated lesion (ALVAL) score [6] and the Natu [36] and Fujishiro [13] grading methods, which semiquantitatively grade the presence/extent of histiocytes, particle types, and tissue

Copyright © 2018 by the Association of Bone and Joint Surgeons. Unauthorized reproduction of this article is prohibited.

Table 3. MRI Protocol for scanning to THA at 1.5 T

	Pulse sequence					
Parameters	**Axial**	**Axial**	**Coronal**	**Sagittal**	**Coronal**	**Coronal**
Acquisition type	FSE	FSE	FSE	FSE	MAVRIC-SL	MAVRIC-SL
Anatomy	Whole pelvis	Hip arthroplasty	Hip arthroplasty	Hip arthroplasty	Whole pelvis	Whole pelvis
Weighting	Intermediate	Intermediate	Intermediate	Intermediate	Intermediate	STIR
Repetition time (ms)	4000-5000	4000-5000	4000-5000	4000-5000	4000-5000	4000-5000
Echo time (ms)	24-34	24-34	24-34	24-34	40	40
Fat suppression	No	No	No	No	No	Inversion pulse at 150 ms
Echo train length	16-24	16-24	16-24	16-24	24	24
Receiver bandwidth (Hz/pixel)	488.3	488.3	488.3	488.3	488.3	488.3
Flip angle (degrees)	90	90	90	90	90	90
Field of view (cm)	36 x 36	26 x 26	26 x 26	26 x 26	44 x 44	44 x 44
Acquisition matrix	512 x 256	512 x 256	512 x 320	512 x 320	512 x 256	512 x 256
Slice thickness (mm)	5	4	4	2.5	3.6	3.6
Section gap (mm)	0	0	0	0	0	0
Number of signals acquired	3	4-5	5	4	0.5	0.5
In-plane frequency direction	S to I	S to I	R to L	A to P	S to I	S to I
Acquisition time (minutes)	5-8	5-8	5-8	5-8	5-7	4-8

FSE = fast-spin echo; MAVRIC = multiacquisition variable resonance image combination; STIR = short T1 inversion recovery; A = anterior; P = posterior; R = right; L = left; S = superior; I = inferior.

particle load. To acknowledge the known limitations of repeatability of the different grading methods [47] and to facilitate subsequent statistical comparisons, each hip was assigned a single overall assessment: acellular membrane = no inflammation with few macrophages; classic ALVAL = diffuse and perivascular lymphocytes, laminated membrane, presence of gray/green particles; particle reaction = macrophages containing particles with minimal perivascular chronic inflammation; extensive necrosis; and infection = five or greater neutrophils in each of five or greater x 400 fields. All grading was performed in a blinded fashion to implant design and preoperative imaging. Gwet's AC1 was used to assess intrarater agreement of overall histologic assessment with almost perfect agreement (AC1, 0.92; 95% CI, 0.85–0.99).

Retrieved polyethylene liners were digitized with a three-dimensional (3-D) laser scanner (range 7; Konica Minolta, Ramsey, NJ, USA) to create 3-D models in Geomagic Qualify (Version 12; Morrisville, NC, USA). Each model was aligned to a sphere the size of the femoral head that had articulated against the liner. Dimensional deviations between the liner model and femoral head model, indicative of wear and/or deformation, were calculated. Volumetric deviations > 285 mm^3 were considered clinically relevant assuming polyethylene manufacturing tolerances of ± 0.14 mm. The head and cup components of selected MoM implants (MoM: n = 5 [14%], HRA: n = 3 [16%]) also underwent contactless scanning (RedLux, Southampton, UK). The selection was based on the availability of retrieved components, the associated MRI classification, and the gross appearance of the retrieved implants. The point clouds were compared with best fit spheres fitted to the unworn portion to calculate linear wear and volumetric wear.

When available, the stem trunnion (male component) or femoral head taper (female component) and articulations of modular neck designs were visually graded for fretting and corrosion [14]. Each trunnion or taper was examined and graded independently by two experienced observers (CE, EB) and categorized as having 1 = none; 2 = mild; 3 = moderate; or 4 = severe fretting or corrosion. Gwet's AC2 was used to assess interrater agreement as well as intrarater agreement of corrosion and fretting the two readers. The analysis found an interrater agreement of moderate to substantial across the features evaluated (AC2 range, 0.60-0.79) and an intrarater agreement of moderate to substantial across the features evaluated (AC2 range, 0.41-0.80).

Copyright © 2018 by the Association of Bone and Joint Surgeons. Unauthorized reproduction of this article is prohibited.

Statistical Analyses

Continuous variables are presented as means with SDs or medians with third and third quartiles. Ordinal variables are presented as medians with first and third quartiles or counts and percentages. Nominal categorical variables are presented as counts and percentages. Continuous variables were compared between more than two groups using analysis of variance or Kruskal-Wallis tests and between pairs of groups using two-sample t-tests or Wilcoxon rank-sum tests. Ordinal variables were compared among more than two groups using Kruskal-Wallis tests and between pairs of groups using Wilcoxon rank-sum tests or Cochran-Armitage trend tests. Nominal categorical variables were compared between groups using chi-square or Fisher's exact tests. Spearman's rank correlation (ρ) was used to assess agreement between continuous and ordinal variables. Probability values < 0.05 were considered to be statistically significant and were adjusted for multiple testing using the Holm-Bonferroni stepdown method. All analyses utilized available data sets (that is, data were not imputed) and were two-sided (SAS Version 9.3; SAS Institute, Cary, NC, USA).

Results

Comparison of MRI Metrics to Implant Type and Histologic Evaluation

Synovial thicknesses differed by implant type (Fig. 2; Table 4), but synovial volume did not. The synovial thickness of metal articulations (MoM: 5.0 [2.8], HRA: 6.1 [2.5]) and modular designs (5.0 [4.0]) displayed no differences in synovial thicknesses ($p = 0.12$) with the patients available, and HRAs had greater synovial thickness than MoP (4.3 [3.7], $p = 0.012$). MoM had greater synovial thickness than CoP (2.8 [1.5], $p = 0.012$). The presence of synovitis differed across the implants ($p = 0.009$) with CoC having less synovitis present (three of six [50%]) as compared with MoM (34 of 35 [97%]) and MoP (55 of 58 [95%]). All implant types, except CoC, presented predominantly (≥ 50%; Table 4) with mixed synovitis. Synovial decompression, or decompression of intraarticular fluid into extraarticular locations, varied by implant type ($p = 0.036$) with the greatest prevalence in patients receiving MoM implants (22 of 35 [63%]). The synovial classification differed by implant type with a greater proportion of MoM classified as ALTR (15 of 35 [43%]) as compared with MoP (nine of 58 [15%], $p < 0.001$), CoP (one of 26 [4%], $p < 0.001$), and CoC (zero of six [0%], $p = 0.009$) hips. The distribution of synovial classification for HRA was not different from MoM. Modular designs had a different distribution of MRI classification compared with MoP ($p < 0.001$) with a greater percentage of modular designs classified as ALTR (20 of 44 [46%]) and MoP classified as polymeric (36 of 58 [62%]). Overall, a greater proportion of MoP was graded, based on MRI, as polymeric (36 of 58 [62%], $p < 0.05$) as compared with MoM (one of 35 [3%]), HRA (zero or 18 [0%]), CoP (seven of 26 [27%]), CoC (one of six [17%]), and modular designs (four of 44 [9%]), whereas metal bearing surfaces (MoM and HRA) and modular designs had a greater proportion graded as ALTR (MoM: 15 of 35 [43%], HRA: 10 of 18 [55%], $p < 0.001$) compared with MoP (nine of 58 [16%]) and CoP (one of 26 [4%]).

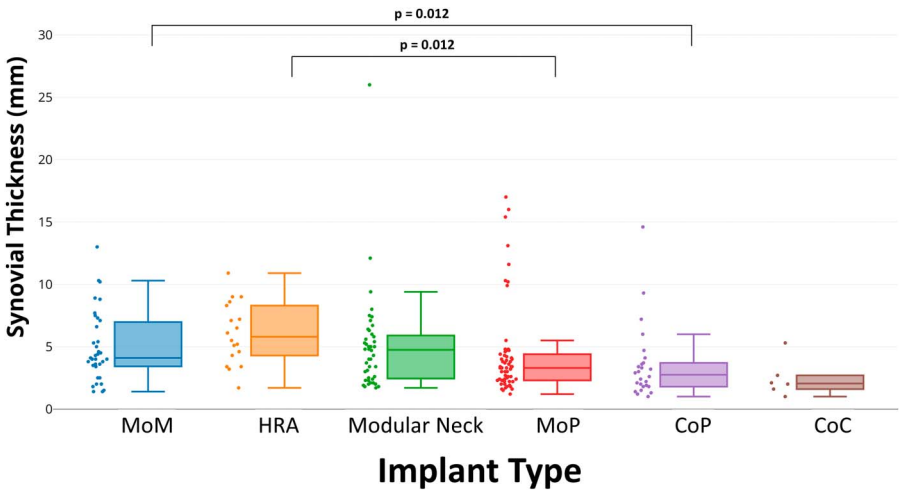

Fig. 2 A box-and-whisker diagram, and associated data points, display that the MRI synovial thickness of HRA implants was greater than MoP designs ($p = 0.012$). In addition, the synovial thickness of MoM designs was greater than the synovial thickness of CoP designs ($p = 0.012$).

Copyright © 2018 by the Association of Bone and Joint Surgeons. Unauthorized reproduction of this article is prohibited.

Table 4. MRI outcome measures

Variable	MoM THA (n = 35)	HRA (n = 18)	Modular designs (n = 44)	MoP THA (n = 58)	CoP THA (n = 26)	CoC THA (n = 6)	p value
Synovial thickness* (mm)	5.0 (2.8)	6.1 (2.5)	5.0 (4.0)	4.3 (3.7)	2.8 (1.5)	2.5 (1.5)	< 0.001
Synovial volume* (cm^3)	42 (48)	41 (57)	52 (134)	51 (83)	23 (34)	10 (20)	0.117
Presence of synovitis							0.009
Present	34 (97%)	17 (94%)	42 (95%)	55 (95%)	26 (100%)	3 (50%)	
Not present	1 (3%)	1 (6%)	2 (5%)	3 (5%)	0 (0%)	3 (50%)	
Type of synovitis							0.002
None	2 (6%)	1 (5%)	2 (4%)	3 (5%)	0 (0%)	3 (50%)	
Fluid	10 (28%)	3 (17%)	7 (16%)	11 (19%)	13 (50%)	2 (33%)	
Fluid + solid (mixed)	23 (66%)	14 (78%)	35 (80%)	44 (76%)	13 (50%)	1 (17%)	
Synovial decompression							0.036
Present	22 (63%)	8 (44%)	26 (59%)	25 (43%)	11 (42%)	0 (0%)	
Not present	23 (37%)	10 (56%)	18 (41%)	33 (57%)	15 (58%)	6 (100%)	
Synovial classification							< 0.001
Normal	3 (9%)	1 (6%)	6 (14%)	6 (10%)	6 (23%)	4 (66%)	
Mildly abnormal	11 (31%)	1 (6%)	11 (25%)	5 (9%)	10 (38%)	1 (17%)	
ALTR	15 (43%)	10 (55%)	20 (45%)	9 (15%)	1 (4%)	0 (0%)	
Infection	0 (0%)	0 (0%)	0 (0%)	1 (2%)	2 (8%)	0 (0%)	
Metallosis	5 (14%)	6 (32%)	3 (7%)	1 (2%)	0 (0%)	0 (0%)	
Polymeric	1 (3%)	0 (0%)	4 (9%)	36 (62%)	7 (27%)	1 (17%)	

*Values displayed as mean (SD); MoM = metal-on-metal; HRA = hip resurfacing arthroplasty; MoP = metal-on-polyethylene; CoP = ceramic-on-polyethylene; CoC = ceramic-on-ceramic; ALTR = adverse local tissue reaction.

MRI synovial thickness differed by histologic classification (Table 5). Acellular membrane (2.3 [1.8-3.9]) had a synovial lining thinner than classic ALVAL (5 [3.5-7.1]), $p < 0.0001$) and extensive necrosis (10.3 [4.8-15.4], $p = 0.004$). Extensive necrosis had the greatest synovial thickness (Fig. 3) and larger than particle reaction (3.3 [2.1–4.6], $p = 0.003$). Classic ALVAL had a larger MRI synovial thickness than particle reaction ($p < 0.001$; Fig. 3). MRI synovial volume differed by histologic classification (Fig. 4) with acellular membrane (4 [2–9]) having the least synovial volume present across all histologic classifications. Extensive necrosis had the greatest synovial volume (163 [78–225]) and was larger than classic ALVAL (33 [12–71], $p = 0.019$) and particle reaction (14 [3–38], $p = 0.009$). Classic ALVAL had greater synovial volume than particle reaction ($p = 0.019$). Weak to moderate positive correlations (Table 6) were found for MRI ALTR grade and synovial thickness with Fujishiro lymphocyte layers ($\rho = 0.43$ [95% CI, 0.30-0.55]; $p < 0.001$, $n = 168$ and $\rho = 0.35$ [95% CI, 0.21-0.47]; $p < 0.001$, $n = 168$, respectively). A greater degree of nonmetallic particle load (Fujishiro) was found for hips classified as polymeric on MRI; however, a greater degree of metal particles (Fujishiro) was not found for hips that had low signal intensity on MRI.

Analysis of MRI Synovial Response by Wear and Corrosion

MRI synovial thickness correlated with severity of fretting and corrosion damage of the female head-neck trunnion of femoral stems in modular designs ($\rho = 0.26$ [95% CI, 0.12-0.39]; $p = 0.015$, $n = 185$). Severity of MRI ALTR grade correlated with the severity of fretting and corrosion damage of the female head-neck trunnion of femoral stems in modular designs ($\rho = 0.30$ [95% CI, 0.01-0.54]; $p = 0.04$, $n = 48$) as well as severity of visible damage (that is, scratching and pitting) on the bearing surface of retrieved femoral heads ($\rho = 0.23$ [95% CI, 0.09-0.36]; $p = 0.001$, $n = 185$). Differences in level of severity of corrosion and fretting on retrieved femoral heads were detected across MRI classifications of synovium (Table 7). In addition, differences in the distribution of severity of corrosion and fretting on retrieved femoral heads and femoral tapers were found by the presence of low signal intensity deposits on MR images. Less corrosion and fretting was associated with MRI synovial classification normal, mildly abnormal, or polymeric, whereas greater corrosion and fretting was associated with a higher prevalence of low signal intensity deposits on MRI (Table 7). In 10 MoM bearings measured for volumetric wear, increasing severity of MRI ALTR grade correlated with higher volumetric wear on the femoral head (Table 8;

Copyright © 2018 by the Association of Bone and Joint Surgeons. Unauthorized reproduction of this article is prohibited.

Table 5. MRI outcomes by histologic classification

Variable	Histologic classification					p value
	Acellular membrane (n = 36)	Classic ALVAL (n = 55)	Extensive necrosis (n = 10)	Infection (n = 9)	Particle reaction (n = 71)	
MRI synovial thickness* (mm)	2.3 (1.8-3.9)	5 (3.5-7.1)†	10.3 (4.8-15.4)	4.1 (3-5)	3.3 (2.1-4.6)	< 0.001
MRI synovial volume* (cm^3)	4 (2-9)	33 (12-71)†	163 (78-225)	21 (19-26)	14 (3-38)	< 0.001
Presence of synovitis						0.21
Not present	3 (8%)	0 (0%)	0 (0%)	0 (0%)	5 (7%)	
Present	33 (92%)	55 (100%)	10 (100%)	9 (100%)	66 (93%)	
Type of MRI synovitis						< 0.001
None	3 (8%)	1 (2%)	0 (0%)	0 (0%)	5 (7%)	
Fluid	23 (64%)	8 (15%)	1 (10%)	1 (11%)	13 (18%)	
Mixed	10 (28%)	46 (84%)	9 (90%)	8 (89%)	53 (75%)	
MRI classification						< 0.001
Normal	13 (36%)	0 (0%)	1 (10%)	1 (11%)	10 (14%)	
Mildly abnormal	17 (47%)	13 (24%)	0 (0%)	0 (0%)	8 (11%)	
ALTR	3 (8%)	26 (47%)	6 (60%)	4 (45%)	14 (20%)	
Infection	1 (3%)	0 (0%)	0 (0%)	1 (11%)	1 (1%)	
Metallosis	0 (0%)	13 (24%)	0 (0%)	0 (0%)	2 (3%)	
Polymeric	2 (6%)	3 (6%)	3 (30%)	3 (33%)	36 (51%)	

*Values of synovial thickness and synovial volume displayed as median (interquartile range).
†two hips did not have data available for analysis; ALVAL = aseptic lymphocyte-dominated vasculitis-associated lesion.

ρ = 0.93 [95% CI, 0.72-0.98]; p < 0.001) and higher volumetric wear on the acetabular component (ρ = 0.89 [95% CI, 0.06-0.99]; p = 0.041). Volumetric femoral head wear was positively correlated with the presence of histiocytes (Natu score, ρ = 0.75 [95% CI, 0.22-0.94]; p = 0.011), particle load (Natu score, ρ = 0.79 [95% CI, 0.31-0.95]; p = 0.005), and metal particles (Fujishiro score, ρ = 0.72 [95% CI, 0.17-0.93]; p = 0.015).

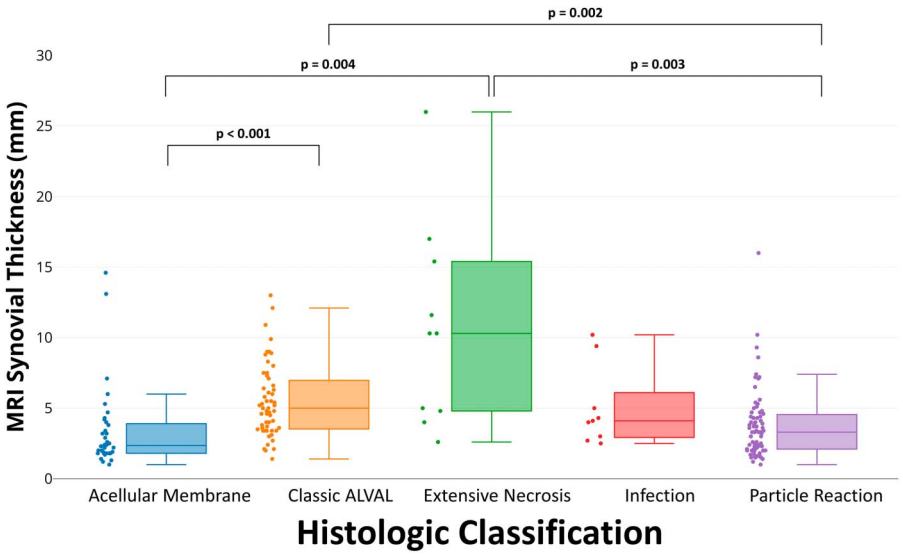

Fig. 3 A box-and-whisker diagram, and associated data points, display that the MRI synovial thickness by the histologic classification of acellular membrane was thinner than classic ALVAL (p < 0.001) and extensive necrosis (p = 0.004). In addition, extensive necrosis had a greater synovial thickness than particle reaction (p = 0.003), and classic ALVAL had a larger synovial thickness than the classification of particle reaction (p = 0.002).

Copyright © 2018 by the Association of Bone and Joint Surgeons. Unauthorized reproduction of this article is prohibited.

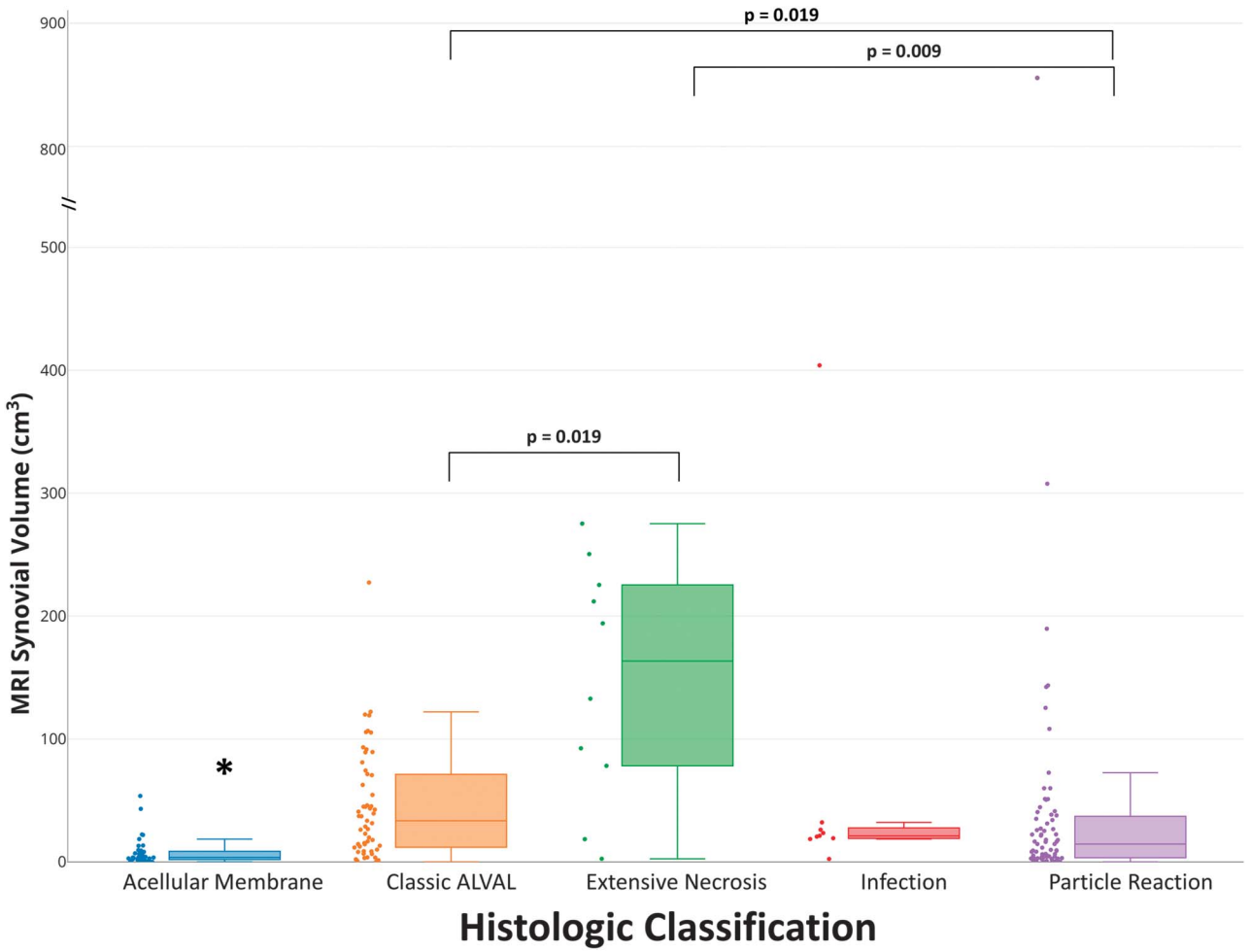

Fig. 4 A box-and-whisker diagram, and associated data points, display that the MRI synovial volume of the acellular membrane classification had the least synovial volume across all histologic categories (*p < 0.013), and extensive necrosis had a synovial volume larger than the classifications of classic ALVAL (p = 0.019) and particle reaction (p = 0.009). In addition, classic ALVAL had a greater MRI synovial volume than particle reaction (p = 0.019).

Discussion

Clinical outcomes of THA are largely successful; however, the generation of wear debris and corrosion products has been implicated in severe ALTRs. Prior studies used MRI to noninvasively evaluate ALTRs, but correlations between the MRI outcomes and clinically or biologically relevant findings were not performed. We correlated indirect MRI findings with direct assessment of implant wear and intraoperative and histologic

Table 6. Correlates of MRI outcomes with histologic measures

MRI variable*	Histologic variable†	Number	Spearman correlation	95% confidence interval		p value
ALTR grading	Natu: particles	167	0.01	-0.14	0.16	0.906
ALTR grading	Fujishiro: other particles	168	-0.11	-0.26	0.04	0.152
ALTR grading	Fujishiro: metal particles	167	0.09	-0.06	0.24	0.259
ALTR grading	Fujishiro: lymph layers	168	0.43	0.30	0.55	< 0.001
Synovial thickness (mm)	Fujishiro: lymph layers	168	0.35	0.21	0.47	< 0.001

*The range of ALTR grading was (none, mild, moderate, or severe).
†the range of all histologic variables was 0 to 4 [8, 23]; ALTR = adverse local tissue reaction.

Copyright © 2018 by the Association of Bone and Joint Surgeons. Unauthorized reproduction of this article is prohibited.

Table 7. Distribution of visual assessment of corrosion and fretting by MRI evaluation

	MRI Classification						
Variable	**Normal**	**Mildly abnormal**	**ALTR**	**Infection**	**Metallosis**	**Polymeric**	**p value**
Visual damage score femoral head	(n = 26)	(n = 39)	(n = 55)	(n = 3)	(n = 14)	(n = 48)	< 0.001
None	23 (88%)	26 (67%)	32 (58%)	2 (66%)	4 (29%)	41 (85%)	
Mild	2 (8%)	11 (28%)	21 (38%)	1 (50%)	8 (57%)	7 (15%)	
Moderate	0 (0%)	2 (5%)	2 (4%)	0 (0%)	1 (7%)	0 (0%)	
Severe	1 (4%)	0 (0%)	0 (0%)	0 (0%)	1 (7%)	0 (0%)	
	Presence of low signal intensity deposits on MRI						
	No	Yes					
Visual damage score femoral head	(n = 146)	(n = 39)					0.001
None	112 (77%)	16 (41%)					
Mild	29 (20%)	21 (54%)					
Moderate	4 (3%)	1 (3%)					
Severe	1 (1%)	1 (3%)					
Visual damage score femoral taper	(n = 144)	(n = 38)					0.001
None	79 (55%)	12 (32%)					
Mild	46 (32%)	12 (32%)					
Moderate	6 (4%)	5 (13%)					
Severe	13 (9%)	9 (24%)					

ALTR = adverse local tissue reaction.

assessment of the surrounding soft tissue. Our results indicate that in our patient population, MRI, evaluated without knowledge of the bearing construct, is capable of distinguishing synovial responses related to macroscopic and microscopic evidence of wear. Although weak correlations were found between MRI synovial thickness or ALTR grade with visual implant damage, stronger correlations were found between MRI and implant volumetric wear. In addition, moderate correlations were found between MRI and histology with the MR grading protocol able to distinguish major patterns of synovial response. Although strong correlations were found between volumetric wear and serum ion levels, MRI has the distinct advantage of directly visualizing the synovial reaction and determining the degree of attendant soft tissue damage, because patients may demonstrate elevated ion levels but not mount an inflammatory reaction to the wear debris.

Table 8. Volumetric wear and deviation measurements

Variable	**MoM THA**	**HRA**	**Modular designs**	**MoP THA**	**CoP THA**
Polyethylene volumetric deviation (mm^3)			38.0 (20.0-62.0) n = 3 (7%)	23.0 (14.0-39.0) n = 15 (26%)	42.0 (14.0-66.0) n = 7 (27%)
Acetabular cup volumetric wear (mm^3)	5.1 (0.2-10) n = 2 (6%)	3.0 (0.0-12.0) n = 3 (16%)			
Acetabular liner volumetric wear (mm^3)	25.0 (0.2 - 99.0) n = 3 (9%)				
Femoral head volumetric wear (mm^3)	24.0 (0.6-42.0) n = 5 (14%)	8 (0.0-54.0) n = 3 (16%)			

Values displayed as median (interquartile range) with number of samples included in the analysis (percentage of total number of hips); MoM = metal-on-metal; HRA = hip resurfacing arthroplasty; MoP = metal-on-polyethylene; CoP = ceramic-on-polyethylene.

Copyright © 2018 by the Association of Bone and Joint Surgeons. Unauthorized reproduction of this article is prohibited.

This study had several limitations. First, the goals of this study required an assessment of implant wear and corrosion and could only be accomplished by requiring the participants to be indicated for revision surgery. Therefore, this study could not determine the rate change in the prevalence of ALTRs as related to wear and corrosion, but only provides evaluation at a single time point across different implant designs. Future studies may be performed that focus on the longitudinal assessment of a painful arthroplasty to determine appropriate clinical followup measures. Second, we did not evaluate specific arthroplasty design factors such as head size and manufacturer or risk factors common in revision of total joint arthroplasty such an anteversion or inclination angles or the association between LOI/reason for revision and synovial volume or similar metrics. We anticipate that implants with larger heads may produce more wear debris and could display a corresponding larger synovial thickness and synovial volume when using MRI as well as a larger particle load from corresponding histology in many cases. However, a strength of the study is that our methods and findings, a one-to-one evaluation of appearance on MRI to implant wear and corrosion through histologic and biomechanical evaluation, were not specific to one particular implant design, primary bearing surface, or level of modularity. MRI provides a noninvasive means to evaluate the synovial and soft tissue response from THAs independent of implant manufacturer or operative technique.

Third, the sampling for assessment of blood serum ions was performed within our institution and these methods do not utilize needles or syringes confirmed to be free of metallic contamination that could have confounded the resulting chromium levels [31]. In addition, glass tubes were used for specimen sampling rather than plastic vials, which could lead to leaching of trace amount of metals into the samples [31]. However, we believe the effects to be minimal because the serum levels of nonmodular THAs and THA without metal-on-metal bearing surfaces displayed little to no presence of cobalt or chromium (Table 2).

Fourth, the methods of MRI, histologic, and corrosion assessment used in the study are subject to assessment bias by the individuals performing the evaluations. The training and experience of each of the examiners could have affected the results and the interpretations of our findings. A repeatability analysis was performed for the qualitative MRI, histologic, and corrosion grading metrics to determine the intra- and interexaminer level of agreement. The results found moderate to almost perfect agreement for each of the analyses performed. Although the levels of agreement for corrosion are similar to what has been reported [19], the MRI grading methods have a higher level of agreement than what has been reported when evaluating MoM constructs [48] ($\kappa = 0.43$ using [2], $\kappa = 0.44$ using [18], and $\kappa = 0.49$ using [33]) and histologic evaluation using original and modified ALVAL scores for patients undergoing MoM THA [47] (intraclass correlation coefficient, 0.38-0.5 and less for individual parameters). We acknowledge the different compositions of implant types in our subject sample, in which we included constructs that contained polyethylene and ceramics; however, the measures of better repeatability could also be attributable to assignment of an overall category rather than assessment of a unique score or measurement. In addition, our category assignment methods are applicable to different implant constructs and not reserved for a single implant design such as MoM or HRA.

Fifth, the results may have been affected by a limited number of samples included in the analysis, even with the appropriate post hoc statistical analyses performed. We sought to perform RedLux scanning for all metal-on-metal bearing surfaces, but the devices were not available as a result of the legal proceedings associated with MoM bearing constructs as well as the cost associated with the scanning technique. We note the large 95% CIs associated with linear and volumetric wear measurements and believe that future studies would benefit from a larger number of sampled specimens. The methods of tissue sampling could have also influenced the lack of additional, or stronger, correlations with histology. Tissue sampling locations were decided based on preoperative MRI. Identifying the exact location from MRI in the operating room proved challenging. Newer MRI analysis techniques could be more sensitive to evaluate regional magnetic field perturbations in the presence of metallic deposits [22]. Future work would benefit from tissue samples acquired around the periphery of all THA articulations as well as tissue-based assays that can classify particle composition with greater accuracy than light microscopy.

The analysis found that not all MRI metrics differed by implant type. Relating our results to other studies is challenging because large cohort MRI studies have not been performed for direct comparison of outcomes across MoM, HRA, MoP, CoP, and CoC constructs, but instead have focused on individual implant constructs such as HRA [9, 39] and MoM [38, 39] or modular versus nonmodular constructs [34]. Furthermore, prior studies that correlated MRI findings with qualitative or quantitative assessment of wear or corrosion focused on MoM bearing surfaces (MoM [38, 39] or HRA [39]) or modular MoP designs [37] with few studies evaluating traditional MoP [27, 52], CoP, or CoC constructs. A recent study focused on corrosion at the taper in patients undergoing MoP THA and utilized preoperative imaging [27] but lacked the detailed MRI evaluation performed in this study or a qualitative assessment of corrosion. Another study used MRI to evaluate HRAs [9] but used a grading system [2] with no clinical correlate. Others utilized preoperative MRI for corrosion in MoP

Copyright © 2018 by the Association of Bone and Joint Surgeons. Unauthorized reproduction of this article is prohibited.

[52], but the implant corrosion was not graded and the MRIs were only assessed for lesion presence and solidity with no further analysis performed. One prior study performed MRI, histologic, and wear evaluation of patients undergoing MoP THA [40], but all patients were indicated for revision as a result of ALTR on MRI (eight of nine with MRI [89%] graded as "severe") and eight of 10 (80%) patients with tissue samples had an ALVAL score ≥ 8. In contrast, only nine of 58 (15%; Table 4) patients undergoing MoP THA in the current study had an ALTR on MRI. In general, these prior studies found that ALTRs do exist in nonmetal articulation constructs, ALVAL scores are higher as compared with non-ALTR comparison groups, and that serum ion levels may also be elevated.

Our results also found differences in histologic classifications by MRI metrics. Again, comparison of our results to prior studies is challenging because each hip was given a single overall assessment for statistical analysis. ALVAL scores [6] are commonly used for histologic grading of ALTRs in patients undergoing MoM [42], modular MoP [25, 49], and MoP [10] THA, but the grading method was shown to only display fair to moderate repeatability [47]. The repeatability of our histologic evaluation displayed near perfect intraexaminer agreement. Our wear measurements compare favorably to a prior report of femoral head and acetabular cup wear measurements [42]. The HRA and MoM femoral head volumetric wear is within the reported 61st and 91st percentiles, respectively, indicating that the MoM samples from our cohort tended to have greater wear present at the time of revision. The acetabular volumetric wear for both MoM and HRA are within the 66th percentile of the previous report. Direct comparison of the polyethylene deviation to previous studies is difficult, because only one prior study used a similar method but only reported the linear wear and not volumetric deviation [8].

We recognize that the MRI classification of the synovium may be challenging, but the interrater examination of this method resulted in substantial to near perfect agreement, which is similar, if not better, than previous reports on the reliability MR-based grading systems for ALTRs [2, 50]. These results highlight the uniformity of assigning synovial classifications by different readers. We purposely enrolled all participants who met inclusion undergoing revision, regardless of bearing surface, implant size, and clinical indication for that revision, to assess the ability of MRI to detect specific synovial patterns across all bearing surfaces.

The MR grading found that the morphologic factors of synovial thickness and volume differed by type of synovitis with the largest thickness and volume found in patients with mixed synovitis. The relationships between the MR metrics and synovial classifications with wear analysis also provided a means of validating items detected on MRI.

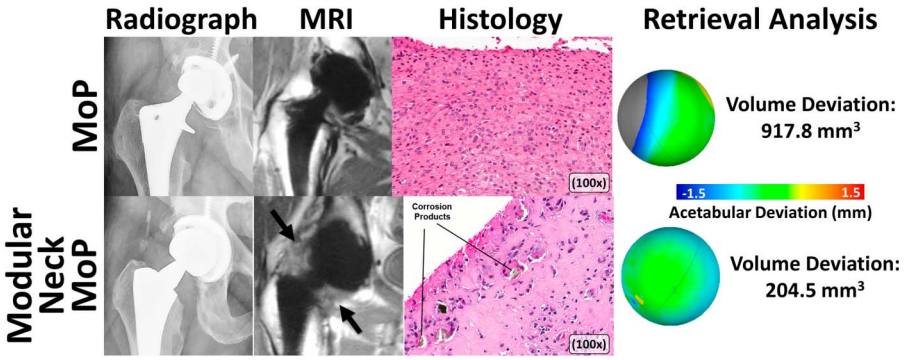

Fig. 5 A montage of images is used to display the full assessment of MoP THAs performed in this study, including preoperative imaging (MAVRIC-SL imaging), intraoperative tissue sampling (hematoxylin and eosin staining), and postoperative wear evaluation. A traditional MoP design (first row, 68-year-old man, femoral stem: VerSys® [Zimmer, Warsaw, IN, USA], femoral head: cobalt-chrome [Zimmer], acetabular component: Harris-Galante [Zimmer], LOI: 20 years) displayed an eccentric femoral head in the polyethylene liner that produced a mild polymeric reaction in the synovium on the MR images. The corresponding histologic assessment displayed sheets of macrophages indicative of polyethylene particles, which corresponded to a large volumetric deviation measured on the polyethylene liner. In contrast to the MoP THA, a modular neck MoP THA design is shown on the second row (54-year-old woman, femoral stem: Rejuvenate [Stryker, Kalamazoo, MI, USA], femoral head: cobalt-chrome [Stryker], acetabular component: Trident [Stryker], LOI: 1.9 years). The MR images displayed a markedly thickened synovial reaction and ALTR (arrows) that correlated to corrosion products at the modular interfaces identified in the corresponding histology as well as the minimal volumetric deviation measured on the polyethylene liner.

Copyright © 2018 by the Association of Bone and Joint Surgeons. Unauthorized reproduction of this article is prohibited.

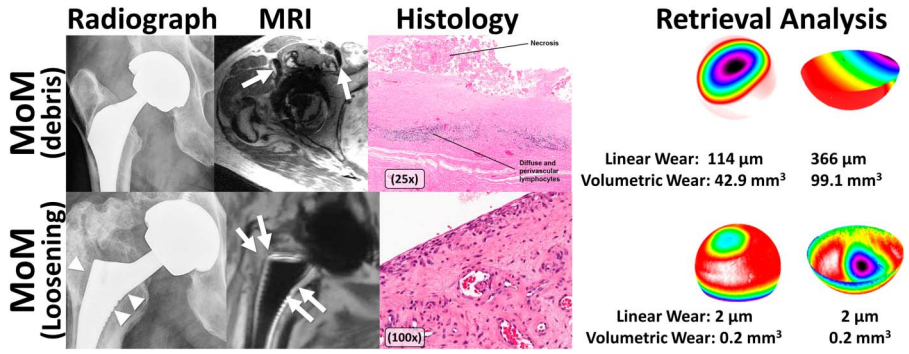

Fig. 6 A montage of images is used to display the full assessment of MoM THA performed in this study, including preoperative imaging (MAVRIC-SL imaging), intraoperative tissue sampling (hematoxylin and eosin staining), and postoperative wear evaluation. The MoM THA on the first row (67-year-old man, femoral stem: unknown design, femoral head: cobalt-chrome [DePuy, Warsaw, IN, USA], acetabular component: Pinnacle® [DePuy], LOI: 9.8 years) displays evidence of low signal intensity deposits on transverse MR images (arrows) that corresponded to necrotic tissue and perivascular lymphocytes typical of ALVAL as displayed in the corresponding histology in addition to moderate linear and volumetric wear as measured on the femoral head and acetabular cup. In contrast to the high wear MoM, another MoM THA is displayed on the second row (52-year-old man, femoral stem: Corail® [DePuy], femoral head: cobalt-chrome [DePuy], acetabular component: Pinnacle [DePuy], LOI: 5.2 years). The MR images show evidence of stem loosening on MR (arrows) as does the corresponding radiograph (arrowheads). The histologic evaluation found no synovial reaction, which also correlated to limited wear on the retrieved components.

Previous MRI classification methods have been based on display characteristics of the ALTR and lacked a direct clinical correlate [2, 18].

We also found that MRI displayed synovial responses, confirmed by histologic evaluation, which are unique to specific implant constructs. An MRI classification of

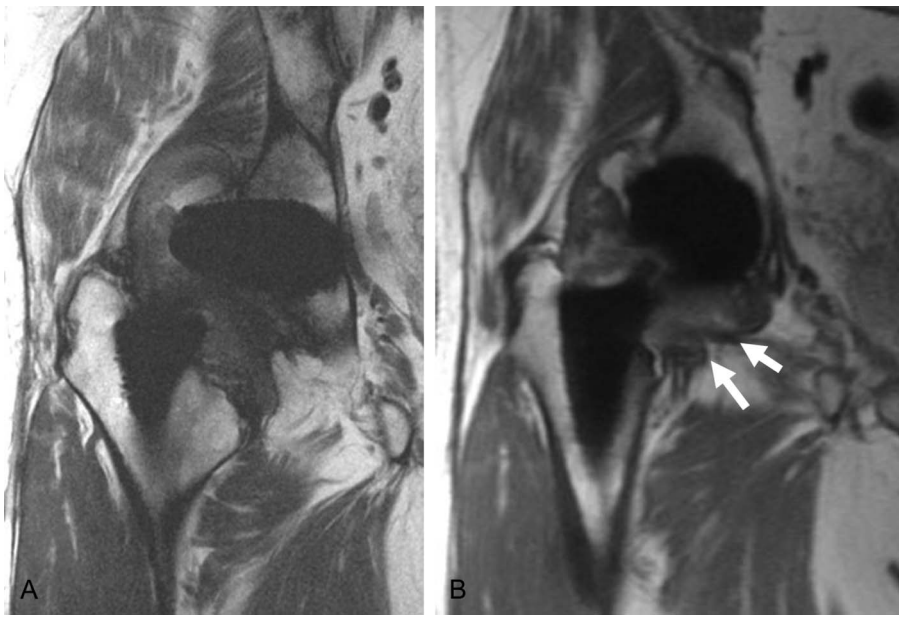

Fig. 7 A-B The MR images of an enrolled patient with an MoP implant displays a thick synovium (17 mm), but low blood serum ion levels (cobalt [Co] = 1.8 ppm and chromium [Cr] = 1.4 ppm) were present. The coronal fast-spin echo image (**A**) and MAVRIC-SL (**B**) images display increased synovial thickness (arrows), indicative of an ALTR confirmed by histologic scores with tissue obtained at the time of revision.

Copyright © 2018 by the Association of Bone and Joint Surgeons. Unauthorized reproduction of this article is prohibited.

polymeric (Fig. 5) was predominantly seen in MoP constructs and corresponded to tissue samples that displayed copious macrophages, indicative of the classic host-mediated polyethylene response. In addition, synovial tissues with the MRI classification of ALTR were predominantly MoM or modular constructs (Fig. 6). We noted that the modular designs presented with MRI features of ALTR including synovial thickness that were also commonly seen in MoM but not in MoP constructs. These results indicate that the interfaces at the head-neck and/or neck-stem junctions are the likely dominant factors of ALTR on MRI. These results correspond well to a previous report of a recalled modular MoP that found corrosion on all tapers at the neck-stem junction [37].

For patients with unilateral THA, serum ion levels were elevated in THAs with MoM articulations. However, the weak to moderate correlations of the serum ion levels with MRI indicate the variability of utilizing a systemic metric such as ion levels to assess tissues around THA. Furthermore, the utility of serum ion levels was limited for a group of patients with low serum ion (< 7 ppb) but with exceedingly large synovial thicknesses. This finding was not just isolated to MoM articulations but was also found in patients with MoP, indicating that trunnion design factors may adversely affect fretting and corrosion, as shown for a representative patient with an MoP implant (Fig. 7). Our results are in agreement with a previous study [32] in not only demonstrating that ion levels may be an insufficient screening mechanism for ALTRs in patients receiving MoM implants, but also that using serum ion levels to evaluate corrosion may not be applicable to other THA designs. Metal ions provide an assessment of implant wear, but MRI has the advantage of noninvasively and directly visualizing the magnitude of the variable host response and potential soft tissue damage.

In this study, we found that MRI provides a means of direct, noninvasive visualization of the patient's synovial response to the implanted hip arthroplasty. The methods of MRI, histologic, and corrosion evaluation used in this study were previously documented in the relevant literature. Although contactless scanning of implants performed in this study required highly specialized equipment, the methods used for MRI, histology, and corrosion evaluation can be implemented using information routinely acquired as part of standard of care examination of a patient at an individual institution. In general, MRI may be used to evaluate patients who present with painful arthroplasty to aid in identifying the cause of discomfort, specifically to highlight any concerning synovial reactions that would warrant more prompt surgical intervention. An MRI that displays a chronic polymeric reaction with focal osteolysis may indicate careful observation, whereas an MRI that displays intracapsular ALTR likely warrants early revision before the process has spread to the abductors and adjacent soft tissue envelope with its attendant soft tissue destruction. In the absence of abnormal host-mediated synovial responses, the MRI can also evaluate for other conditions causing pain, including abductor and psoas tendinopathy, stress reactions/occult fractures, and cup impingement. In recalled implants or those at risk for ALTR/metallosis, the MRI can be used to screen for clinically silent ALTR in asymptomatic patients.

Furthermore, we anticipate these methods may be used to assess new THA constructs in the future, similar to what was performed for modular neck THA and the associated early revision for this implant design. Future studies that utilize MRI to prospectively evaluate different implant designs will be necessary to assess the longitudinal natural history of arthroplasty complications, including the development and prevalence of ALTR across bearing constructs and component integration. It would also be beneficial to integrate the influence of mixed metal taper junctions [29] and flexural rigidity [21] in the development of ALTRs.

This current comprehensive analysis correlates noninvasive MRI measures with biologically relevant histologic analyses and direct measures of wear. These data illustrate the value of MRI as a diagnostic tool to evaluate THA, having a positive impact on the management of patients at risk for revision surgery.

Acknowledgments We thank Ms Bin Lin for her assistance in the preparation of the manuscript, Dr Alissa J. Burge for her assistance with repeatability of MRI evaluation, and the Hospital for Special Surgery Adult Reconstruction and Joint Replacement Service for assistance in acquiring intraoperative tissue samples for the study.

References

1. Amstutz HC, Grigoris P. Metal on metal bearings in hip arthroplasty. *Clin Orthop Relat Res*. 1996;329(Suppl):S11-34.
2. Anderson H, Toms AP, Cahir JG, Goodwin RW, Wimhurst J, Nolan JF. Grading the severity of soft tissue changes associated with MOM hip replacements: reliability of an MR grading system. *Skeletal Radiol*. 2011;40:303-307.
3. Barlow BT, Boles JW, Lee YY, Ortiz PA, Westrich GH. Short-term outcomes and complications after rejuvenate modular total hip arthroplasty revision. *J Arthroplasty*. 2016;31:857-862.
4. Bragdon CR, Doerner M, Martell J, Jarrett B, Palm H, Multicenter Study Group, Malchau H. The 2012 John Charnley Award: Clinical multicenter studies of the wear performance of highly crosslinked remelted polyethylene in THA. *Clin Orthop Relat Res*. 2013;471:393-402.
5. Campbell J, Rajaee S, Brien E, Paiement GD. Inflammatory pseudotumor after ceramic-on-ceramic total hip arthroplasty. *Arthroplast Today*. 2017;3:83-87.
6. Campbell P, Ebramzadeh E, Nelson S, Takamura K, De Smet K, Amstutz HC. Histological features of pseudotumor-like tissues from metal-on-metal hips. *Clin Orthop Relat Res*. 2010;468:2321-2327.
7. Campe CB, Palmer WE. MR imaging of metal-on-metal hip prostheses. *Magn Reson Imaging Clin N Am*. 2013;21:155-168.

Copyright © 2018 by the Association of Bone and Joint Surgeons. Unauthorized reproduction of this article is prohibited.

8. Carli A, Koch CN, Esposito CI, Wright TM, Padgett DE. Polyethylene wear increases in liners articulating with scratched oxidized zirconium femoral heads. *Clin Orthop Relat Res*. 2018; 476:182-192.
9. Connelly JW, Galea VP, Matuszak SJ, Madanat R, Muratoglu O, Malchau H. Indications for MARS-MRI in patients treated with metal-on-metal hip resurfacing arthroplasty. *J Arthroplasty*. 2018;33:1919-1925.
10. Cooper HJ, Della Valle CJ, Berger RA, Tetreault M, Paprosky WG, Sporer SM, Jacobs JJ. Corrosion at the head-neck taper as a cause for adverse local tissue reactions after total hip arthroplasty. *J Bone Joint Surg Am*. 2012;94:1655-1661.
11. D'Antonio JA, Sutton K. Ceramic materials as bearing surfaces for total hip arthroplasty. *J Am Acad Orthop Surg*. 2009;17:63-68.
12. Esposito CI, Wright TM, Goodman SB, Berry DJ; Clinical, Biological and Bioengineering Study Groups from Carl T. Brighton Workshop. What is the trouble with trunnions? *Clin Orthop Relat Res*. 2014;472:3652-3658.
13. Fujishiro T, Moojen DJ, Kobayashi N, Dhert WJ, Bauer TW. Perivascular and diffuse lymphocytic inflammation are not specific for failed metal-on-metal hip implants. *Clin Orthop Relat Res*. 2011;469:1127-1133.
14. Goldberg JR, Gilbert JL, Jacobs JJ, Bauer TW, Paprosky W, Leurgans S. A multicenter retrieval study of the taper interfaces of modular hip prostheses. *Clin Orthop Relat Res*. 2002;401:149-161.
15. Goldsmith AA, Dowson D, Isaac GH, Lancaster JG. A comparative joint simulator study of the wear of metal-on-metal and alternative material combinations in hip replacements. *Proc Inst Mech Eng H*. 2000;214:39-47.
16. Hart AJ, Sabah S, Henckel J, Lewis A, Cobb J, Sampson B, Mitchell A, Skinner JA. The painful metal-on-metal hip resurfacing. *J Bone Joint Surg Br*. 2009;91:738-744.
17. Hart AJ, Satchithananda K, Liddle AD, Sabah SA, McRobbie D, Henckel J, Cobb JP, Skinner JA, Mitchell AW. Pseudotumors in association with well-functioning metal-on-metal hip prostheses: a case-control study using three-dimensional computed tomography and magnetic resonance imaging. *J Bone Joint Surg Am*. 2012;94:317-325.
18. Hauptfleisch J, Pandit H, Grammatopoulos G, Gill HS, Murray DW, Ostlere S. A MRI classification of periprosthetic soft tissue masses (pseudotumours) associated with metal-on-metal resurfacing hip arthroplasty. *Skeletal Radiol*. 2012;41:149-155.
19. Hothi HS, Matthies AK, Berber R, Whittaker RK, Skinner JA, Hart AJ. The reliability of a scoring system for corrosion and fretting, and its relationship to material loss of tapered, modular junctions of retrieved hip implants. *J Arthroplasty*. 2014;29: 1313-1317.
20. Jacobs JJ, Hallab NJ, Skipor AK, Urban RM. Metal degradation products: a cause for concern in metal-metal bearings? *Clin Orthop Relat Res*. 2003;417:139-147.
21. Kao YY, Koch CN, Wright TM, Padgett DE. Flexural rigidity, taper angle, and contact length affect fretting of the femoral stem trunnion in total hip arthroplasty. *J Arthroplasty*. 2016;31: 254-258.
22. Koch KM, Koff MF, Bauer TW, Shah PH, Nencka AS, Sivaram Kaushik S, Potter HG. Off-resonance based assessment of metallic wear debris near total hip arthroplasty. *Magn Reson Med*. 2018;79:1628-1637.
23. Koch KM, Lorbiecki JE, Hinks RS, King KF. A multispectral three-dimensional acquisition technique for imaging near metal implants. *Magn Reson Med*. 2009;61:381-390.
24. Koff MF, Shah P, Koch KM, Potter HG. Quantifying image distortion of orthopedic materials in magnetic resonance imaging. *J Magn Reson Imaging*. 2013;38:1083-1091.
25. Kolatat K, Perino G, Wilner G, Kaplowitz E, Ricciardi BF, Boettner F, Westrich GH, Jerabek SA, Goldring SR, Purdue PE. Adverse local tissue reaction (ALTR) associated with corrosion products in metal-on-metal and dual modular neck total hip replacements is associated with upregulation of interferon gamma-mediated chemokine signaling. *J Orthop Res*. 2015;33: 1487-1497.
26. Kwon YM, Ostlere SJ, McLardy-Smith P, Athanasou NA, Gill HS, Murray DW. 'Asymptomatic' pseudotumors after metal-on-metal hip resurfacing arthroplasty: prevalence and metal ion study. *J Arthroplasty*. 2011;26:511-518.
27. Lachiewicz PF, O'Dell JA. Trunnion corrosion in metal-on-polyethylene hip arthroplasty. *Bone Joint J*. 2018;100:898-902.
28. Langton DJ, Joyce TJ, Jameson SS, Lord J, Van Orsouw M, Holland JP, Nargol AV, De Smet KA. Adverse reaction to metal debris following hip resurfacing: the influence of component type, orientation and volumetric wear. *J Bone Joint Surg Br*. 2011;93:164-171.
29. Langton DJ, Sidaginamale RP, Joyce TJ, Meek RD, Bowsher JG, Deehan D, Nargol AVF, Holland JP. A comparison study of stem taper material loss at similar and mixed metal head-neck taper junctions. *Bone Joint J*. 2017;99:1304-1312.
30. Lu W, Pauly KB, Gold GE, Pauly JM, Hargreaves BA. SEMAC: slice encoding for metal artifact correction in MRI. *Magn Reson Med*. 2009;62:66-76.
31. MacDonald SJ, Brodner W, Jacobs JJ. A consensus paper on metal ions in metal-on-metal hip arthroplasties. *J Arthroplasty*. 2004;19:12-16.
32. Macnair RD, Wynn-Jones H, Wimhurst JA, Toms A, Cahir J. Metal ion levels not sufficient as a screening measure for adverse reactions in metal-on-metal hip arthroplasties. *J Arthroplasty*. 2013;28:78-83.
33. Matthies AK, Skinner JA, Osmani H, Henckel J, Hart AJ. Pseudotumors are common in well-positioned low-wearing metal-on-metal hips. *Clin Orthop Relat Res*. 2012;470: 1895-1906.
34. Mikkelsen RT, Flojstrup M, Lund C, Kjaersgaard-Andersen P, Skjodt T, Varnum C. Modular neck vs nonmodular femoral stems in total hip arthroplasty–clinical outcome, metal ion levels, and radiologic findings. *J Arthroplasty*. 2017;32:2774-2778.
35. Morozov PP, Sana M, McGrory BJ, Farraher SW, Abrahams TG. Comparison of pre-revision magnetic resonance imaging and operative findings in mechanically assisted crevice corrosion in symptomatic metal-on-polyethylene total hip arthroplasties. *J Arthroplasty*. 2017;32:2535-2545.
36. Natu S, Sidaginamale RP, Gandhi J, Langton DJ, Nargol AV. Adverse reactions to metal debris: histopathological features of periprosthetic soft tissue reactions seen in association with failed metal on metal hip arthroplasties. *J Clin Pathol*. 2012; 65:409-418.
37. Nawabi DH, Do HT, Ruel A, Lurie B, Elpers ME, Wright T, Potter HG, Westrich GH. Comprehensive analysis of a recalled modular total hip system and recommendations for management. *J Bone Joint Surg Am*. 2016;98:40-47.
38. Nawabi DH, Gold S, Lyman S, Fields K, Padgett DE, Potter HG. MRI predicts ALVAL and tissue damage in MoM hip arthroplasty. *Clin Orthop Relat Res*. 2014;472:471-481.
39. Nawabi DH, Nassif NA, Do HT, Stoner K, Elpers M, Su EP, Wright T, Potter HG, Padgett DE. What causes unexplained pain in patients with metal-on metal hip devices? A retrieval, histologic, and imaging analysis. *Clin Orthop Relat Res*. 2014;472: 543-554.
40. Nodzo SR, Esposito CI, Potter HG, Ranawat CS, Wright TM, Padgett DE. MRI, retrieval analysis, and histologic evaluation of

Copyright © 2018 by the Association of Bone and Joint Surgeons. Unauthorized reproduction of this article is prohibited.

adverse local tissue reaction in metal-on-polyethylene total hip arthroplasty. *J Arthroplasty*. 2017;32:1647-1653.
41. Pandit H, Glyn-Jones S, McLardy-Smith P, Gundle R, Whitwell D, Gibbons CL, Ostlere S, Athanasou N, Gill HS, Murray DW. Pseudotumours associated with metal-on-metal hip resurfacings. *J Bone Joint Surg Br*. 2008;90:847-851.
42. Park SH, Lu Z, Hastings RS, Campbell PA, Ebramzadeh E. Five hundred fifty-five retrieved metal-on-metal hip replacements of a single design show a wide range of wear, surface features, and histopathologic reactions. *Clin Orthop Relat Res*. 2018;476: 261-278.
43. Plodkowski AJ, Hayter CL, Miller TT, Nguyen JT, Potter HG. Lamellated hyperintense synovitis: potential MR imaging sign of an infected knee arthroplasty. *Radiology*. 2013;266:256-260.
44. Potter HG, Nestor BJ, Sofka CM, Ho ST, Peters LE, Salvati EA. Magnetic resonance imaging after total hip arthroplasty: evaluation of periprosthetic soft tissue. *J Bone Joint Surg Am*. 2004;86:1947-1954.
45. Sabah SA, Mitchell AW, Henckel J, Sandison A, Skinner JA, Hart AJ. Magnetic resonance imaging findings in painful metal-on-metal hips: a prospective study. *J Arthroplasty*. 2011;26: 71-76, 76.e1-2.
46. Sieber HP, Rieker CB, Kottig P. Analysis of 118 second-generation metal-on-metal retrieved hip implants. *J Bone Joint Surg Br*. 1999;81:46-50.
47. Smeekes C, Cleven AHG, van der Wal BCH, Dubois SV, Rouse RW, Ongkiehong BF, Wolterbeek R, Nelissen R. Current pathologic scoring systems for metal-on-metal THA revisions are not reproducible. *Clin Orthop Relat Res*. 2017;475:3005-3011.
48. Smeekes C, Schouten BJM, Nix M, Ongkiehong BF, Wolterbeek R, van der Wal BCH, Nelissen R. Pseudotumor in metal-on-metal hip arthroplasty: a comparison study of three grading systems with MRI. *Skeletal Radiol*. 2018;47:1099-1109.
49. Su SL, Koch CN, Nguyen TM, Burket JC, Wright TM, Westrich GH. Retrieval analysis of neck-stem coupling in modular hip prostheses. *J Arthroplasty*. 2017;32:2301-2306.
50. van der Weegen W, Brakel K, Horn RJ, Wullems JA, Das HP, Pilot P, Nelissen RG. Comparison of different pseudotumor grading systems in a single cohort of metal-on-metal hip arthroplasty patients. *Skeletal Radiol*. 2014;43:149-155.
51. van der Weegen W, Sijbesma T, Hoekstra HJ, Brakel K, Pilot P, Nelissen RG. Treatment of pseudotumors after metal-on-metal hip resurfacing based on magnetic resonance imaging, metal ion levels and symptoms. *J Arthroplasty*. 2014;29:416-421.
52. Whitehouse MR, Endo M, Zachara S, Nielsen TO, Greidanus NV, Masri BA, Garbuz DS, Duncan CP. Adverse local tissue reactions in metal-on-polyethylene total hip arthroplasty due to trunnion corrosion: the risk of misdiagnosis. *Bone Joint J*. 2015; 97:1024-1030.
53. Willert HG, Buchhorn GH, Fayyazi A, Flury R, Windler M, Koster G, Lohmann CH. Metal-on-metal bearings and hypersensitivity in patients with artificial hip joints. A clinical and histomorphological study. *J Bone Joint Surg Am*. 2005;87:28-36.

Copyright © 2018 by the Association of Bone and Joint Surgeons. Unauthorized reproduction of this article is prohibited.